REGULAR ARTICLE

blood advances

Integrated phosphoproteomics and transcriptional classifiers reveal hidden RAS signaling dynamics in multiple myeloma

Yu-Hsiu T. Lin,[1] Gregory P. Way,[2] Benjamin G. Barwick,[3] Margarette C. Mariano,[1] Makeba Marcoulis,[1] Ian D. Ferguson,[1] Christoph Driessen,[4] Lawrence H. Boise,[3] Casey S. Greene,[2,5] and Arun P. Wiita[1]

[1]Department of Laboratory Medicine, University of California, San Francisco, San Francisco, CA; [2]Department of Systems Pharmacology and Translational Therapeutics, University of Pennsylvania, Philadelphia, PA; [3]Department of Hematology and Medical Oncology and Winship Cancer Institute, Emory University, Atlanta, GA; [4]Experimental Oncology and Hematology, Department of Oncology and Hematology, Kantonsspital St. Gallen, St. Gallen, Switzerland; and [5]Childhood Cancer Data Laboratory, Alex's Lemonade Stand Foundation, Philadelphia, PA

Key Points

- *NRAS* and *KRAS* mutations lead to different downstream transcriptional signatures and patient prognoses under current myeloma therapies.
- *RAS* genotype alone does not strongly predict degree of active MAPK signaling, suggesting alternate precision medicine approaches are needed.

A major driver of multiple myeloma (MM) is thought to be aberrant signaling, yet no kinase inhibitors have proven successful in the clinic. Here, we employed an integrated, systems approach combining phosphoproteomic and transcriptome analysis to dissect cellular signaling in MM to inform precision medicine strategies. Unbiased phosphoproteomics initially revealed differential activation of kinases across MM cell lines and that sensitivity to mammalian target of rapamycin (mTOR) inhibition may be particularly dependent on mTOR kinase baseline activity. We further noted differential activity of immediate downstream effectors of Ras as a function of cell line genotype. We extended these observations to patient transcriptome data in the Multiple Myeloma Research Foundation CoMMpass study. A machine-learning–based classifier identified surprisingly divergent transcriptional outputs between *NRAS*- and *KRAS*-mutated tumors. Genetic dependency and gene expression analysis revealed mutated Ras as a selective vulnerability, but not other MAPK pathway genes. Transcriptional analysis further suggested that aberrant MAPK pathway activation is only present in a fraction of *RAS*-mutated vs wild-type *RAS* patients. These high-MAPK patients, enriched for *NRAS* Q61 mutations, have inferior outcomes, whereas *RAS* mutations overall carry no survival impact. We further developed an interactive software tool to relate pharmacologic and genetic kinase dependencies in myeloma. Collectively, these predictive models identify vulnerable signaling signatures and highlight surprising differences in functional signaling patterns between *NRAS* and *KRAS* mutants invisible to the genomic landscape. These results will lead to improved stratification of MM patients in precision medicine trials while also revealing unexplored modes of Ras biology in MM.

Introduction

Multiple myeloma (MM) is an incurable malignancy of plasma cells. Considerable effort has gone into deep sequencing of MM to genomically classify patients for risk assessment and targeted therapy.[1-5] While these studies have offered significant insight into MM biology and prognosis, this genomic knowledge largely remains untranslated into therapeutic strategies.[6]

Submitted 15 April 2019; accepted 23 August 2019. DOI 10.1182/bloodadvances.2019000303.

Mass spectrometry data are accessible from the PRoteomics IDEntifications database under the accession number PXD011551. Phosphoproteomic measurements are available as supplemental Data Set 1. The code used for the supervised machine-learning model in this paper is available at https://zenodo.org/record/2566059#.XHTWgeJKiAM and for the phosphoproteomic analysis and its integration with DepMap at https://github.com/YHTLin/MMCL-phospho.

The full-text version of this article contains a data supplement.

We hypothesized that one reason genomic profiles alone have not improved clinical outcome is that they may not be fully predictive of higher-level processes, such as dysregulated signaling, that drive cancer phenotypes. Mass spectrometry–based phosphoproteomics has therefore proven a powerful tool to explore cellular-wide signaling alterations in cancer.[7,8] For example, studies in acute myeloid leukemia have shown that phosphorylation signatures can be used to predict sensitivity to kinase inhibitors in cell lines and primary samples.[9,10] Alternatively, as an indirect measure of cellular signaling, downstream transcriptional signatures may reveal specific functional readouts of upstream kinase activity.[11]

In MM, it is thought that aberrant signaling is strongly driven by mutations in the *RAS* family of proto-oncogenes. These mutations are proposed to activate oncogenic signaling primarily via the MAPK and phosphatidylinositol 3-kinase (PI3K)/protein kinase B (AKT) pathways.[12,13] An outstanding mystery in oncology is tumor-specific selection of mutations in different *RAS* isoforms, despite >80% sequence homology and highly similar function.[13,14] Furthermore, it is not known why mutations in specific *RAS* codons predominate in some cancers but not others.[15,16]

MM is a unique case study of Ras biology, as ~40% of MM patient tumors have predicted activating mutations in *KRAS* or *NRAS*,[4,5] with an approximately equal distribution between the two. Notably, these mutations are very rare in the precursor lesion monoclonal gammopathy of uncertain significance, suggesting that *RAS* mutations are important for disease transformation.[17] The majority of MM research has treated mutations in these *RAS* isoforms as largely indistinguishable, though some distinctions have emerged. For example, under earlier MM therapies, patients with *KRAS* mutations had worse overall survival than those with *NRAS* mutations.[18,19] However, later observations suggested that patients with *NRAS* mutations responded more poorly to bortezomib-based therapies than patients with *KRAS* mutations.[20] Cell line studies indicated that *KRAS* leads to more rapid proliferation in the absence of interleukin-6 stimulation than *NRAS*.[21,22] More recent sequencing studies have suggested that *NRAS* mutations tend to cluster with specific genomic aberrations.[5] Finally, bone marrow immunohistochemistry suggested differences in extracellular signal-regulated kinase (ERK) phosphorylation depending on the *RAS* isoform and specific mutation.[23] Therefore, this evidence suggests that *KRAS* and *NRAS* in MM are not exactly equivalent, but much about the biology of these differences remains unclear.

Here, we apply an integrated approach using both unbiased phosphoproteomics and machine-learning classifiers of transcriptional response to dissect signaling in MM. Our results reveal differential kinase activity across MM cell lines with potential implications for selective kinase vulnerability. We next uncover underlying transcriptional output differences for patients with *KRAS* and *NRAS* mutations, with particular prognostic implications of *NRAS* Q61 mutations. Surprisingly, we find that only a fraction of *RAS*-mutated patients are predicted to have highly activated MAPK signaling vs wild-type (WT) *RAS* patients. Our results identify *RAS*-mutated MM patients who may benefit from precision medicine strategies and reveal modes of *RAS* isoform-driven biology with implications across *RAS*-mutated cancers.

Methods

Cell culture and phosphoproteomics

Cell lines were cultured and phosphoproteomics experiments and analysis were performed as described previously.[24] Additional details can be found in supplemental Methods.

Kinase inhibitor screens on myeloma cell lines

Briefly, 1e3 myeloma cells were seeded per well in a 384-well plate and treated with the designated inhibitor at each dose in quadruplicate. Viability was determined at 48 hours using CellTiterGlo reagent (Promega) and 50% inhibitory concentration calculated using GraphPad Prism software v6. Additional details are available in supplemental Methods.

RAS classifier for MM

We downloaded RNA sequencing (RNA-seq) and somatic mutation data from the Multiple Myeloma Research Foundation (MMRF) CoMMpass (version IA11a); 90% of patient data with transcriptome and genotype information (n = 706) was used to optimize and train the machine-learning classifier, and the remaining 10% of data (n = 80) was withheld as a test set. The data were split to ensure balanced representation of total *KRAS*, *NRAS*, and WT *RAS* samples. We adapted our previously published elastic net penalized logistic regression classifier for predicting *RAS* pathway activation[25] with a one-vs-rest approach to classify *KRAS* and *NRAS* mutations separately. Additional details can be found in supplemental Methods.

MAPK pathway activity and the Multiple Myeloma Kinome Browser

We applied a perturbation-response machine-learning model called PROGENy (https://github.com/saezlab/progeny) implemented in *R* on RNA-seq data from myeloma cell lines (www.keatslab.org) and patient samples (CoMMpass IA11). The MAPK PROGENy score quartiles were compared with patient progression-free survival (PFS) and overall survival (OS) using a Cox proportional hazards regression; score quartiles were compared with patient clinical characteristics (age, sex, race, β2 microglobulin, and M-protein) using a linear regression for continuous variables and Fisher's exact test for discrete variables. Common translocations and copy-number alterations were determined as previously described.[26] Additional details are available in supplemental Methods.

Results

Kinase activity from phosphoproteomics is modestly predictive of kinase inhibitor sensitivity in myeloma cell lines

We first aimed to predict differential kinase activity across MM cell lines and investigated whether increased kinase activity led to increased vulnerability to selective inhibitors. We used immobilized metal affinity chromatography to enrich phosphopeptides across 7 MM cell lines and 1 in vitro–evolved bortezomib-resistant cell line[27] (Figure 1A). In total, 19 155 phosphosites from 4941 proteins were quantified across all cell lines (supplemental Data Set 1; supplemental Table 1). As expected, >99% of all identified phosphorylation events were on Ser or Thr sites.

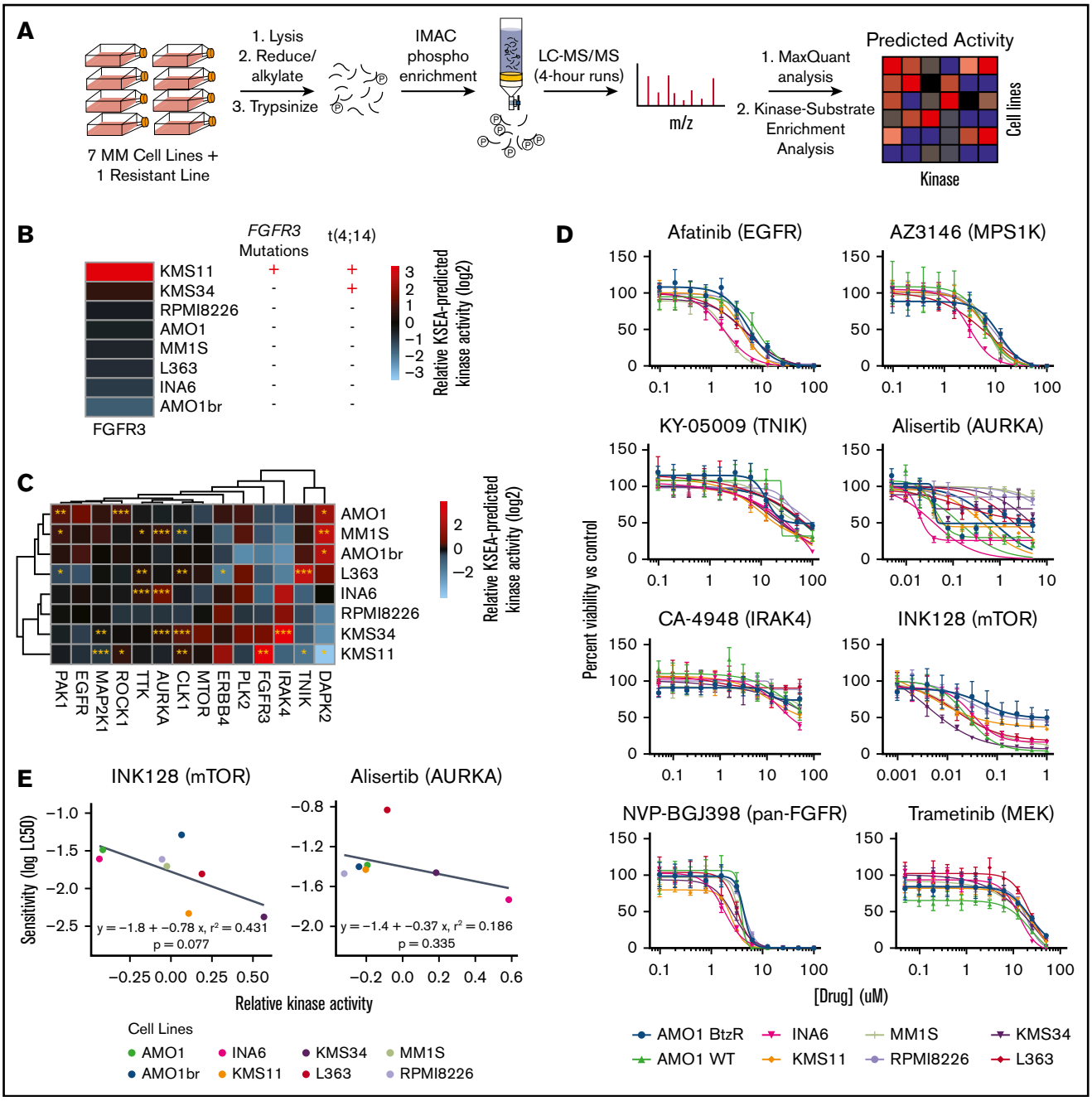

Figure 1. Predicting kinase activity and inhibitor sensitivity in MM by unbiased phosphoproteomics. (A) Schematic of the pipeline for kinase activity prediction from phosphoproteomic data. All phosphoproteomics were performed in biological triplicate and combined by averaging the $\log_2$-transformed intensities of phosphosites associated with each kinase to generate activity scores. (B) Association of predicted FGFR3 activity from KSEA with known genetic aberrations. (C) Heatmap of the KSEA-predicted activities of 14 kinases that exhibited differential activity signatures across myeloma cell lines. The significance of the score from the median activity across cell lines was calculated by z-statistics (see "Methods"). *$P \leq .05$, **$P \leq .01$, ***$P \leq .001$. (D) Viability curves showing the drug response of 8 myeloma cell lines to 8 kinase inhibitors (n = 4, mean ± standard deviation), with only INK128 and alisertib exhibiting strongly differential effects. (E) Correlation between inhibitor sensitivity and KSEA-predicted kinase activity for mTOR and aurora kinase A across myeloma cell lines shows modest predictive power. *P* values were calculated based on the null hypothesis that no relationship exists between the activity of a kinase and its sensitivity to an inhibitor. LC50, 50% lethal concentration; IMAC, immobilized metal affinity chromatography; LC-MS/MS, liquid chromatography-tandem mass spectrometry.

The Pearson *R* of phosphosite intensity correlations within each line ranged from 0.86 to 0.95, underscoring the reproducibility of this analysis (supplemental Figure 1).

We used kinase-substrate enrichment analysis (KSEA)[28] to identify kinases with predicted differential activity in ≥1 cell line vs all others. As an initial validation of KSEA, we found that KMS-11, with both

a t(4;14) translocation and an activating mutation in *FGFR3*, showed the highest predicted activity of FGFR3 kinase (Figure 1B). KMS-34, with a t(4;14) translocation increasing *FGFR3* expression but no *FGFR3* mutation, showed the second-highest predicted FGFR3 activity. Overall, using KSEA, we identified 14 kinases that appeared to have differential activity across MM cell lines (Figure 1C).

We next evaluated whether differential kinase activities predicted sensitivity to inhibitors. Using an initial prescreening on 3 MM lines (AMO-1, MM.1S, and RPMI-8226), we found that 8 of 13 available selective inhibitors demonstrated anti-MM effects at $\leq$20 μM (supplemental Figure 2A). We then tested these inhibitors on all 8 lines used for phosphoproteomics (Figure 1D). We were surprised to find that only 2 of the 8 inhibitors tested in the full panel showed a notable distribution of the lethal concentrations required to kill 50% of the population (LC_{50}s) across the tested MM lines. We more closely examined these inhibitors (alisertib targeting Aurora kinase A and INK128 targeting mammalian target of rapamycin [mTOR] kinase) and found a modest correlation between predicted kinase activity and sensitivity to the inhibitor (Figure 1E). Within the smaller range of LC_{50}s for other inhibitors, we did not find correlations between predicted kinase activity and inhibitor LC_{50}, though we note that KMS-11 and KMS-34 were 2 of the 3 most sensitive lines to the pan-FGFR inhibitor NVP-BGJ398 (supplemental Figure 2B). Overall, these results suggest that kinase activities from KSEA are modestly predictive of sensitivity to targeted kinase inhibitor therapy.

Phosphoproteomics reports on specific alterations in MAPK pathway activity as a function of *RAS* mutation status

As mutations in *RAS* are the most commonly seen single-nucleotide genomic alteration in MM,[5] we next examined the known Ras effectors. The KSEA-predicted activity of the RAF isoforms ARAF, BRAF, and CRAF/RAF1 is reflective of MAPK activation immediately downstream of Ras.[29] We first noted that cell lines with *RAS* mutations did not show uniform RAF isoform activity as inferred by KSEA on our phosphoproteomic data. Instead, the 2 lines (MM.1S and RPMI-8226) with canonical activating mutations in *KRAS* (both G12A) showed the highest levels of predicted BRAF and ARAF activity (Figure 2A). We note that while relative BRAF and CRAF phosphorylation at a single canonical site alone appears largely unchanged across lines, KSEA kinase activity scores reflect aggregate signaling effects across annotated phosphosites on multiple proteins. Similar to findings in other studies,[30] by western blotting, we further found that *RAS* mutation status did not lead to consistent levels of ERK1/2$^{T202/Y204}$, AKT$^{T308/S473}$, and 4EBP1$^{T37/46}$ phosphorylation, commonly used readouts of downstream MAPK and PI3K/AKT activities (Figure 2B).

A machine-learning–based classifier distinguishes transcriptional output of *KRAS* vs *NRAS* mutants in MM patients and cell lines

These findings motivated us to further evaluate the biological differences between *KRAS* and *NRAS* mutations in MM patients. As MM patient samples are not amenable to phosphoproteomics due to sample input limitations, we turned to more widely available transcriptome data. We recently reported a machine-learning classifier based on an elastic net penalized logistic regression able to predict *RAS* genotype, or *RAS*-mutant-like phenotype, from tumor RNA-seq.[25] This initial classifier, trained and tested on solid tumor data from The Cancer Genome Atlas, did not distinguish between *RAS* isoforms. Applying this initial classifier to RNA-seq data from 812 patient tumors in the MMRF CoMMpass study (release IA11a; research.themmrf.org), we observed very limited predictive power for *RAS* genotype (supplemental Figure 3A).

Review of gene weights in the initial *RAS* classifier revealed that many highly weighted genes were expressed minimally in hematopoietic cells (not shown), potentially leading to this lack of applicability. Ras signaling has previously been detected using machine learning applied to a single tumor type.[31] We therefore used a similar machine-learning strategy to build an MM-specific classifier based on CoMMpass patient data. We extended our prior computational approach by developing a 3-way classifier, attempting to distinguish transcriptional signatures of patients with WT *RAS*, *KRAS* mutations, and *NRAS* mutations (Figure 3A). For building the classifier, we included patients in the mutation category if activating *KRAS*/*NRAS* mutations in codon positions 12, 13, and 61 were reported in CoMMpass data, irrespective of variant allele frequency (VAF). Ten patients with subclonal mutations in both *KRAS* and *NRAS* were excluded.

We used 90% of the CoMMpass patient data as a training set (n = 706 total; n = 439 WT, n = 138 *KRAS*, n = 129 *NRAS*) and the remaining 10% (n = 106 total; n = 49 WT, n = 16 *KRAS*, n = 15 *NRAS*) as a holdout test set. The one-vs-rest, multiclass logistic regression classifier was trained to predict *RAS* genotype based on transcriptional signatures in 8000 genes that exhibited the greatest variance in expression across CoMMpass samples. Our classifier performed robustly in both the training and test sets, with areas under the receiver operating characteristic curves between 0.81 and 0.97 in the test set (Figure 3B). We also applied the classifier to a data set of 65 MM cell lines (data from www.keatslab.org). The classifier performed similarly well in these data, indicating high generalizability (supplemental Figure 3B).

We next investigated whether differences exist in predictions between patients carrying *KRAS* and *NRAS* mutations. To address this, we first examined the "confusion matrix," finding that incorrectly predicted *NRAS*-mutant genotype samples in the training set and incorrectly predicted *KRAS*-mutant genotype samples in the testing set were more likely to be predicted as being WT *RAS* rather than a mutation in the other *RAS* isoform (Figure 3C). This finding underscores divergence in transcriptional output between these mutations. We also observed that tumors with higher VAF had less accurate classification between *KRAS* and *NRAS* mutation while lower VAF led to less accurate classification between WT and *RAS* mutant (supplemental Figure 3C). Overall, we found no statistical difference between the clonality of activating *KRAS* and *NRAS* mutations in MM patients (supplemental Figure 3D).

We further examined the highest weighted genes for the *KRAS* mutant, *NRAS* mutant, or WT *RAS* classifiers (Figure 3D; supplemental Data Set 2). We found a limited set of genes whose expression levels increased the probability of classification as either *RAS* mutant and decreased probability of WT *RAS*: *SPRED2*, *GRK6*, *F12*, and *ETV5*. Of these genes, *SPRED2* and *ETV5* are well defined as MAPK responsive.[32,33] Overall, however, the genes that specifically defined an increased or decreased probability of *KRAS* or *NRAS* mutant classification were largely independent of each other (genes along x- and y-axes in Figure 3D). Surprisingly,

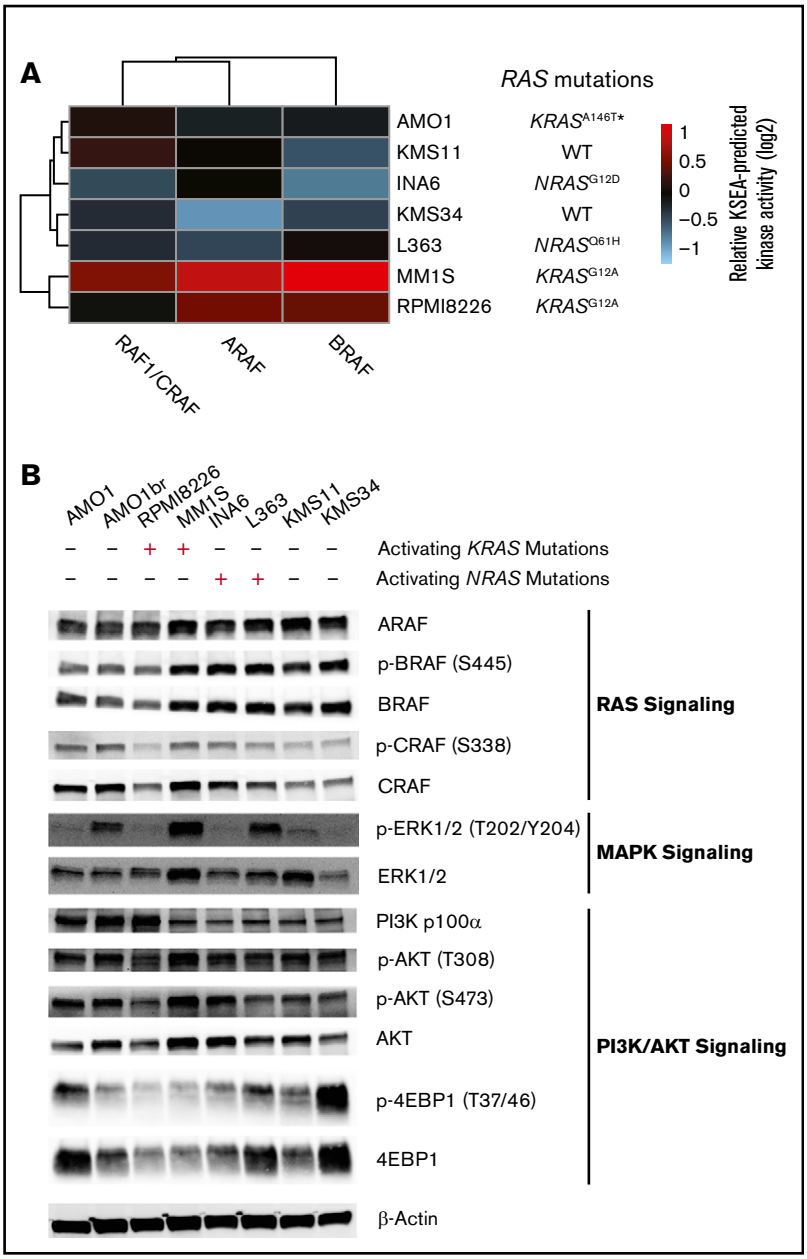

Figure 2. *KRAS* mutant MM cell lines show greatest activation of downstream RAF effectors based on phosphoproteomics. (A) Heatmap of KSEA-predicted activity of the immediate downstream substrates of Ras protein (ARAF, BRAF, and RAF1/CRAF) across the 7 profiled myeloma cell lines. (B) Western blot analysis of RAS, MAPK, and PI3K/AKT pathway signatures in MM cell lines.

the only gene whose expression strongly predicted *NRAS* over *KRAS* mutation was *NRAS* itself.

RAS mutants drive differential expression of *RAS* genes and oncogenic addiction in myeloma

This finding motivated us to further examine *RAS* gene expression as a function of genotype in MM patients. Consistent with our machine-learning classifier, we indeed found that patients with a detected *NRAS* mutation had significantly increased expression of *NRAS* compared with *KRAS*-mutated samples (Figure 4A). We also saw a less pronounced reciprocal relationship in *KRAS*-mutated samples. This finding is reminiscent of that found in a prior analysis of numerous cancer cell lines, where mutations in one *RAS* isoform were associated with increased expression of that isoform and depressed expression of the other.[34] We further confirmed a similar relationship between *NRAS* mutation and gene expression, but not *KRAS*, across MM cell lines (supplemental Figure 4).

We next took advantage of data on "essential genes" required for cell viability as determined via genome-wide short hairpin RNA (shRNA) and clustered regularly interspaced short palindromic repeats (CRISPR) screens.[35] We confirmed earlier single-gene knockdown results[36] that *RAS*-mutated MM cells are highly dependent on the specific *RAS*-mutated isoform (Figure 4B). However, this genome-wide analysis did not identify any other genes across both the shRNA and CRISPR data that led to specific dependency in *NRAS* or *KRAS* mutants or between *RAS*-mutated cell lines and WT *RAS* lines (Figure 4C). These findings underscore the profound "oncogene addiction" of MM plasma cells to mutated *RAS*.

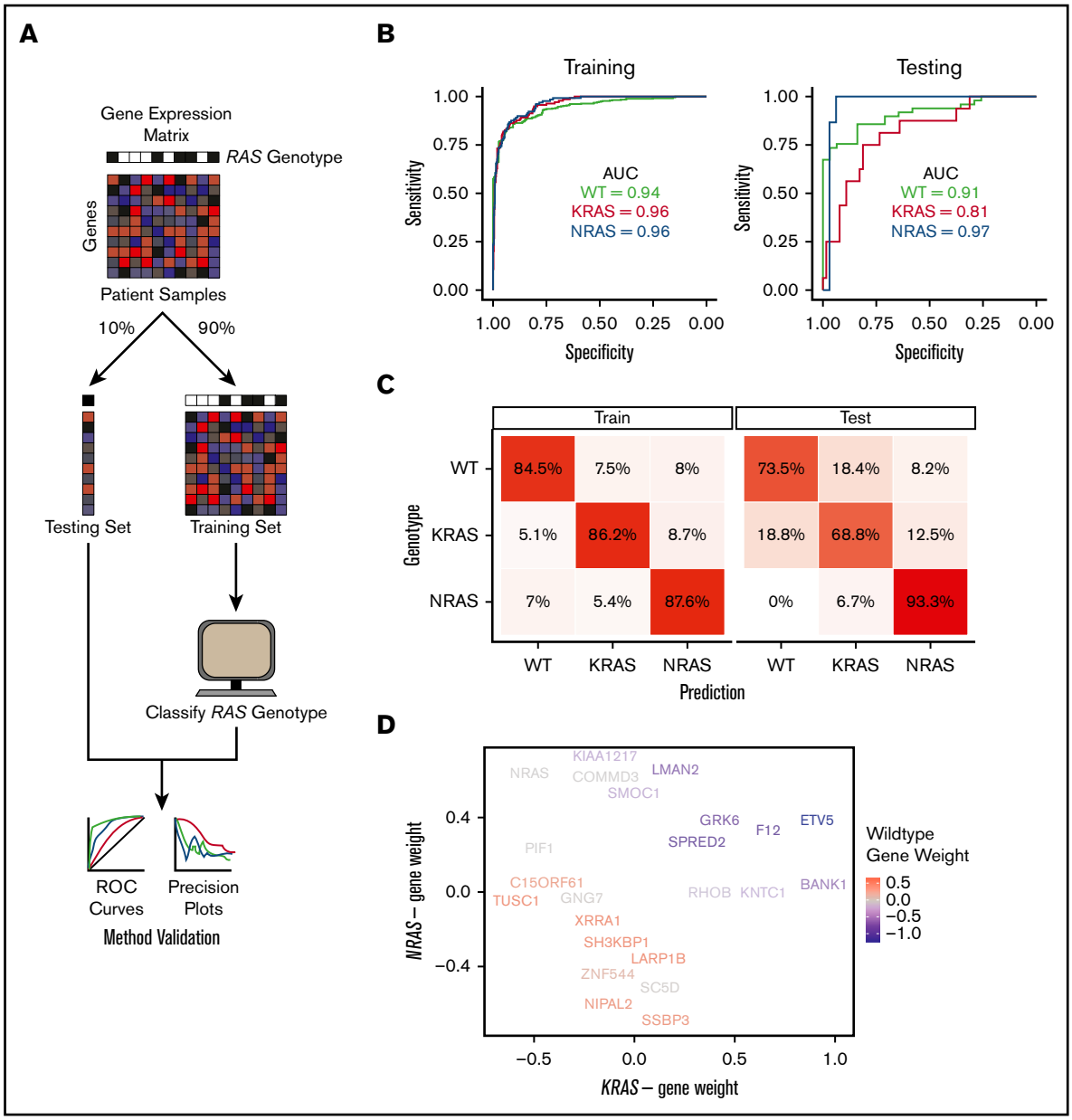

Figure 3. An MM-specific, transcriptome-based *RAS* classifier reveals genes driving the *NRAS* and *KRAS* phenotype. (A) Workflow for training and testing a gene-expression–based machine-learning algorithm to predict *RAS* genotype using an elastic net regression model. (B) Receiver operating characteristic curves for evaluating the performance of the predictive model on the training and testing sets. The area under the curve (AUC) is reported for each prediction class. (C) Confusion matrices showing the fraction of samples in each label-vs-predicted-class combination. (D) Multidimensional plot displaying weighted genes playing the most prominent role in predicting *NRAS*, *KRAS*, or WT *RAS* genotype.

KRAS mutations at any codon and *NRAS* Q61 mutations lead to poorer prognosis

We next examined the relationship between *RAS* mutation and clinical outcomes in CoMMpass. If we included all patients with a detected *RAS* mutation, either at the level of any mutation (VAF >0) or those with a dominant subclone (VAF >0.3), we actually found no effect on either PFS or OS (Figure 5A), consistent with prior studies.[37]

We next looked more specifically at differences in *KRAS* and *NRAS* mutations. We found that cases with *KRAS* mutation at VAF >0 (n = 161) have a significantly decreased PFS vs all others (P = .034), though there was no significant difference in OS (P = .55) (Figure 5B). Surprisingly, for cases with a dominant *KRAS*-mutant subclone (VAF >0.3; n = 83), any relationship with survival difference disappeared (PFS P = .28; OS P = .74).

In contrast, we did not find any outcome effects of all patients with *NRAS* mutations vs all others (supplemental Figure 5A). We next found significantly decreased PFS at VAF >0 (P = .022) and a similar trend at VAF >0.3 (P = .074) for *KRAS* vs *NRAS*-mutated samples but no significant difference in OS (Figure 5C). Overall,

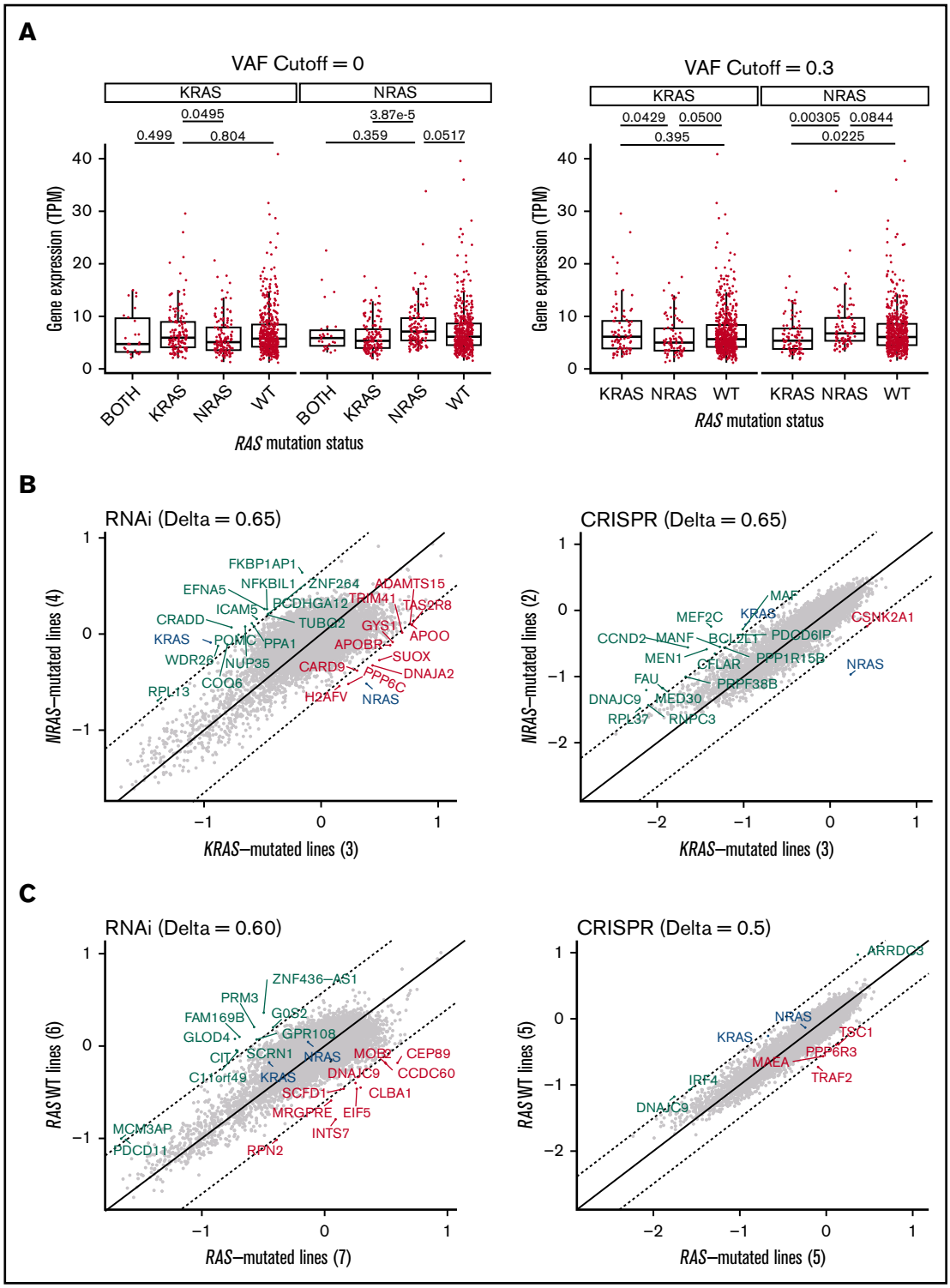

Figure 4. MM-mutant *KRAS* and *NRAS* are associated with differential *RAS* expression and are "addicted" to the mutated *RAS* isoform. (A) Boxplots of *KRAS* and *NRAS* expression in tumor samples from newly diagnosed MM patients in CoMMpass. The distributions are stratified by *RAS* mutation status and VAF to evaluate their effects on gene expression. *P* values from Welch's 2-tailed *t* tests are reported for relevant comparisons. (B) Scatterplot of the gene dependency scores from DepMap between *NRAS*-mutated and *KRAS*-mutated MM cell lines from RNA interference (18Q2 release) or CRISPR deletion (Avana 18Q2) functional screens. Comparing between the two data sets, the related *RAS* gene shows consistent essentiality, but not other genes. Dashed lines represent cutoffs (Δ) for differential gene dependency between the *RAS*-mutated lines. (C) Similar to panel B, comparing WT *RAS* and *RAS*-mutated myeloma cell lines.

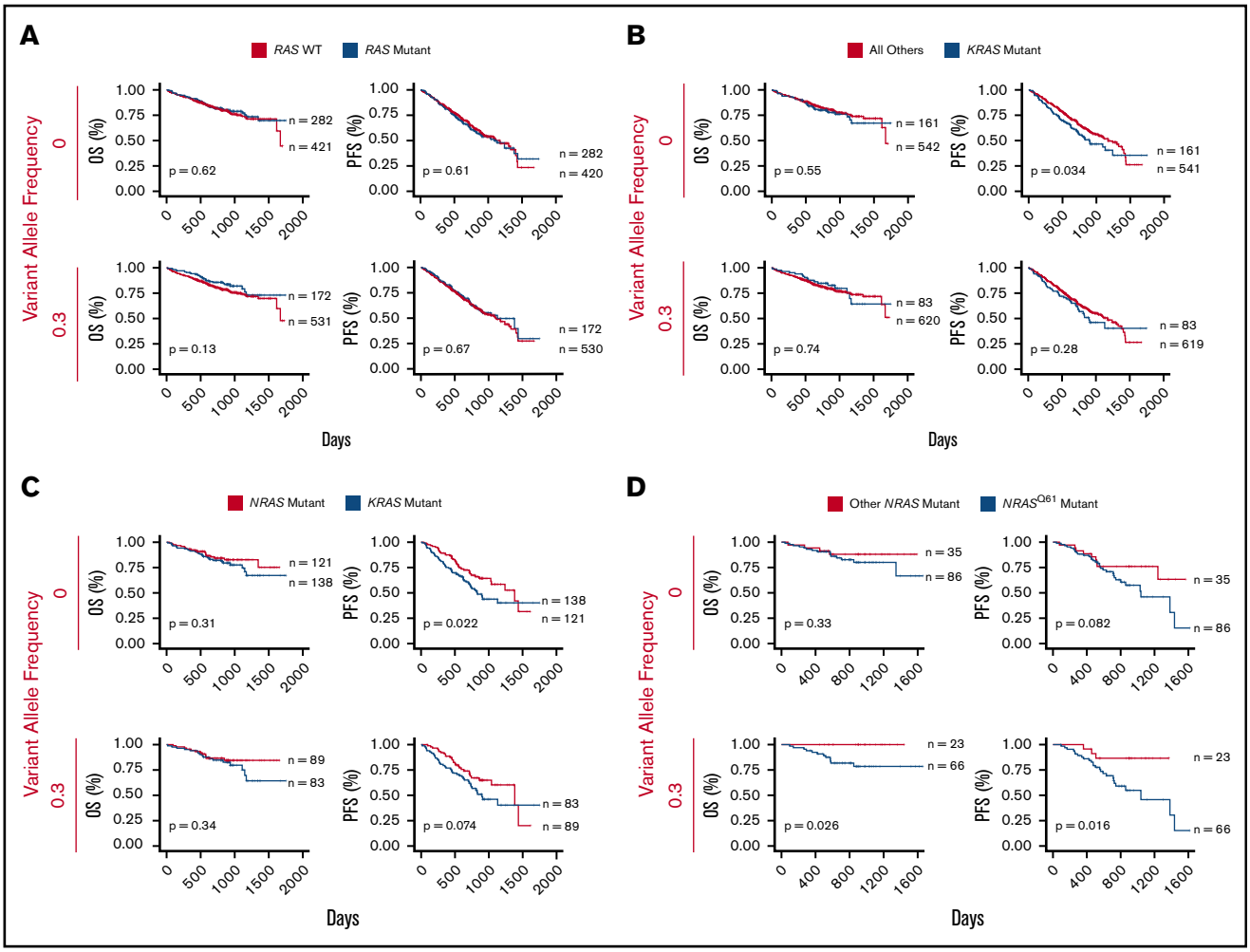

Figure 5. *KRAS* mutations and *NRAS* Q61 predict worse outcomes in MM. (A) Survival curves comparing the clinical outcome of newly-diagnosed MM patients with and without activating *RAS* mutations (CoMMpass release IA11). (B) *KRAS*-mutated MM patients vs all other patients. (C) Activating *KRAS* vs *NRAS* mutations. (D) Codon-61 *NRAS* mutations vs other *NRAS* variants. All analyses were performed at VAF cutoffs of 0 and 0.3 to assess the effect of tumor heterogeneity on survivorship, with 0.3 as a signifier of a largely dominant *RAS*-mutated clone for this heterozygous mutation. *P* values from log-rank test and the sample size for each group are reported.

these findings appear somewhat consistent with earlier results, suggesting that *KRAS* mutations carry a worse prognosis than *NRAS* mutations,[18,19] though with modern treatment regimens, this poor-prognosis effect of *KRAS* is perhaps not as pronounced.

We next looked at specific effects of activating mutations[13] in codons 12, 13, and 61. We did not find significant differential survival effects for *KRAS* mutations in any specific codon (supplemental Figure 5D-F). However, *NRAS* mutations at codon Q61 led to strikingly worse PFS and OS vs other *NRAS* mutations, but only when present in a dominant subclone (PFS $P = .016$ and OS $P = .026$ at VAF >0.3) (Figure 5D). This finding suggests that clonal or near-clonal *NRAS* Q61 mutations are particularly potent in driving disease in the setting of current therapies.

A perturbation-based transcriptional signature identifies highly variable activation of the MAPK pathway across *RAS* mutant samples

Our results thus far strongly suggest that *NRAS* and *KRAS* mutants are not equivalent in driving MM. We next examined functional readouts of MAPK pathway activation in the context of *RAS* mutation. We took advantage of a recently described method of transcriptional classification of pathway activity termed PROGENy.[38] This method provides improved prediction of pathway activation when compared with prior methods of transcriptional analysis.[38] Using PROGENy prediction for MAPK pathway activity, we were surprised to find a very prominent overlap of MAPK activation scores across *RAS*-mutated patients vs WT *RAS* (Figure 6A). This result stands in contrast to the expected finding of clearly increased MAPK activity in *RAS*-mutated patients vs WT *RAS*, which, notably, we found in MM cell lines (Figure 6B). Despite this large degree of overlap in patient samples, we still found that the mean of the MAPK distribution was significantly increased for both *KRAS* ($P = 2.16e-6$) and *NRAS* mutants ($P = .0123$), as well as rare patients with mutations in both genes ($P = 1.53e-4$), vs WT *RAS*. Overall, however, our results suggest that many patients with *RAS* mutations do not strongly activate the MAPK pathway over patients with WT *RAS* tumors.

Examining codon-level effects (Figure 6C) for *KRAS*, we found no significant differences between MAPK scores for mutations in

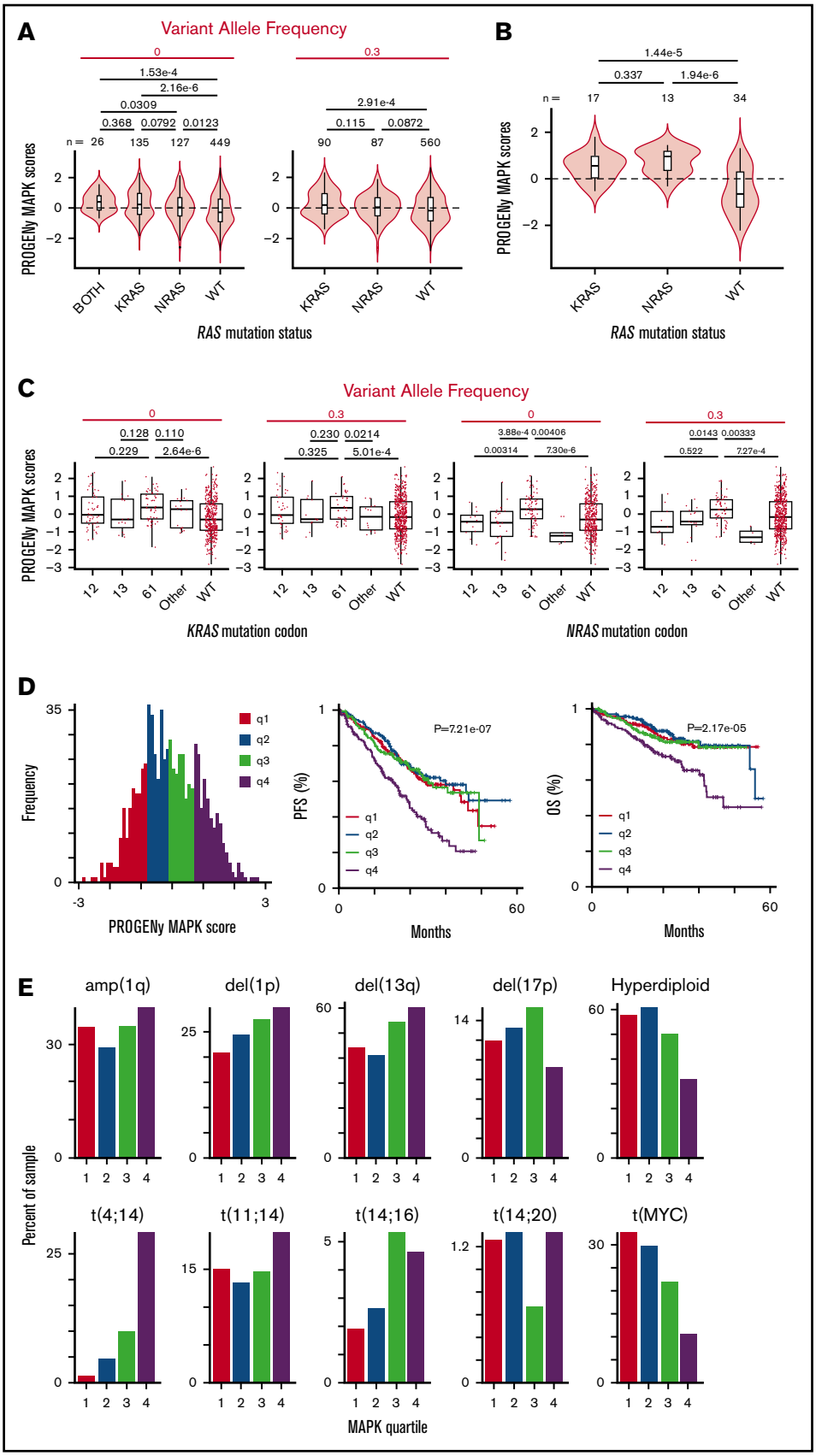

Figure 6. PROGENy reveals *RAS* mutations do not strongly increase MAPK activity in all *RAS*-mutant tumors, but patients with increased MAPK activity have decreased survival. (A) Violin plots showing the distribution of MAPK pathway activation for MM patient samples in CoMMpass based on PROGENy predictions reveals a surprisingly similar range of scores for WT *RAS* and *RAS*-mutated patients, though mean of distribution is significantly different. *P* values for all combinations using Welch's 2-tailed *t* tests. (B) MM cell lines (data from www.keatslab.org) show more pronounced effects of *RAS* mutation driving MAPK activity than patient samples in panel A. (C) Activating mutations at the Q61 codon show the strongest effect in driving MAPK activity in *NRAS* mutants in CoMMpass samples, whereas *KRAS* mutations do not show similar codon-specific effects. *P* values by Welch's 2-tailed *t* test. (D) Histogram of PROGENy-predicted MAPK activation colored by quartiles. Survival analyses demonstrate that high levels of MAPK activity are predictive of poorer outcomes. *P* values were calculated using Wald's test. (E) Association between PROGENy-predicted MAPK scores and common genomic markers in MM.

codons 12, 13, and 61. For *NRAS*, in contrast, we found significantly higher MAPK scores for mutations in codon 61 vs codons 12 and 13. MAPK scores were also markedly higher for codon 61 vs rare mutations in other noncanonical *NRAS* codons in patients.

Increased MAPK activity predicts worse patient outcomes

These observations led us to hypothesize that high levels of tumor MAPK pathway activity, regardless of *RAS* mutation status, may manifest in more aggressive disease. Consistent with our hypothesis, we indeed found that patients in the highest quartile MAPK score had significantly decreased PFS ($P = 7.21e\text{-}7$) and OS ($P = 2.17e\text{-}5$) (Figure 6D).

We sought to rule out the possibility that an increased MAPK score served as a proxy for known prognostic features in MM. We did not find any relationship between MAPK score and sex, race, age, or β2 microglobulin, though we identified an association with increased M-protein at diagnosis (supplemental Figure 6A). We next evaluated the relationship between MAPK score and MM genomic subtypes (Figure 6E). We found a significant relationship between MAPK score and t(4;14) translocation,[39] consistent with the ability of FGFR-family tyrosine kinases to activate MAPK upstream of Ras.[40] We also observed more limited associations with other poor prognosis features such as del(1p) and del(13q) (Figure 6E; supplemental Figure 6B). We further evaluated the relationship between MAPK score and common sequence variants present in >2% of CoMMpass patients (supplemental Figure 6C; supplemental Data Set 3), finding a significant association with *FGFR3*, *KRAS*, and *BRAF* mutations, but not *NRAS*. Together, these results confirm MAPK-related genomic lesions can lead to increased MAPK activity, consistent with known biology. However, these results also underscore the limitation of genome-only testing; a majority of patients with these well-characterized changes are not in the top quartile of MAPK activity associated with poor prognosis. Overall, our results support the transcriptome-based PROGENy MAPK score as a differential predictor of MM outcomes from other previously known biochemical or genomic markers.

Integrated analysis of kinase activity and drug sensitivity informs precision medicine in MM

Our results suggest that targeting therapies specifically for patients with increased MAPK activity, as opposed to *RAS* genotype alone, may be a fruitful strategy in MM precision medicine. To suggest agents which may be most effective in this context, we analyzed data from the Genomics of Drug Sensitivity in Cancer database.[41] Of 265 total compounds tested, we identified 3 small molecules, the MEK inhibitor refametinib, the MEK inhibitor PD0325901, and the BRAF inhibitor dabrafenib, that showed the greatest correlation ($R^2 > 0.65$; supplemental Figure 7) between the Genomics of Drug Sensitivity in Cancer IC_{50}s in MM cell lines ($n = 15$) and PROGENy MAPK scores from transcriptome data (Figure 7A). These agents could be potentially considered in clinical applications with targeted use based on tumor transcriptome-based MAPK score.

To assist in further integration of kinase activity into precision medicine, we developed an interactive software tool called the Multiple Myeloma Kinome Browser (https://tony-lin.shinyapps.io/depmap_app/) combining our phosphoproteome-based kinase activity predictions with multiple data types on MM cell lines from the Cancer Dependency Map (18Q2 release). We integrated functional studies, such as drug sensitivity, CRISPR deletion, and shRNA screens, with features including gene expression, copy-number variation, and mutations, for 297 kinases across seven MM cell lines. As one example of its use, we show that a strong, negative association exists between the predicted activity and the sensitivity of checkpoint kinase 1 to 2 different Chk1 inhibitors (Figure 7B). This freely available resource may prove beneficial for future investigation of targeted therapies in MM.

Discussion

Here, we used an integrated approach of unbiased phosphoproteomics and transcriptional classifiers to identify differential regulation of signaling in MM. Our results delineate prominent differences in *KRAS* and *NRAS* signaling outputs, biology, and patient outcomes.

Notably, only 2 of 13 inhibitors we tested showed any notable correlation between predicted kinase activity and sensitivity. For INK128 (TAK-228/sapanasertib), a phase 1/2 trial in MM showed only minimal responses to single-agent therapy.[42] Our data suggest that selecting patients based on mTOR pathway activation may lead to better results for other mTOR inhibitors, such as the newly described molecule RapaLink-1.[43] Some of the lack of predictive power of our phosphoproteome analysis is likely biological; simply because a specific kinase activity is increased does not mean a tumor will selectively depend on it for survival. We are also limited by current bioinformatics tools, which are imperfect in predicting kinase activity across thousands of phosphopeptides.[44]

We next shifted our focus to *RAS*. Both in MM cell lines and primary samples, there has been surprisingly little correlation between MAPK activity as measured by ERK phosphorylation and sensitivity to tested MEK/ERK inhibitors.[30,45] We also found no relationship between predicted MEK activity and sensitivity to the MEK inhibitor trametinib (Figure 1D). Immunohistochemistry of MM patient bone marrow has suggested that the majority shows ERK phosphorylation, regardless of *RAS* mutation status.[46] These findings suggest that ERK phosphorylation is not a specific readout of MAPK activity that drives tumor aggression. Broader transcriptional signatures, such as those we derive here, could be more effective in identifying patients who could benefit from targeted therapies.

By adapting a machine-learning classifier,[25] we demonstrated that mutated *NRAS* and *KRAS* are associated with divergent downstream transcriptional signatures. The relationship between *RAS* mutation status and gene expression may align with emerging evidence of allelic imbalance across oncogenes, where both mutation status and gene expression converge to drive tumor proliferation.[47,48] These findings further elucidate underlying biological differences among these Ras isoforms in MM that were not previously observed.

Our finding that patients with the highest predicted PROGENy MAPK scores carry the poorest prognosis leads to a pressing question: is there a way to exploit this observation for MM precision medicine? Our results strongly support the notion that genotype alone is not enough to stratify MM patients to receive MEK or ERK

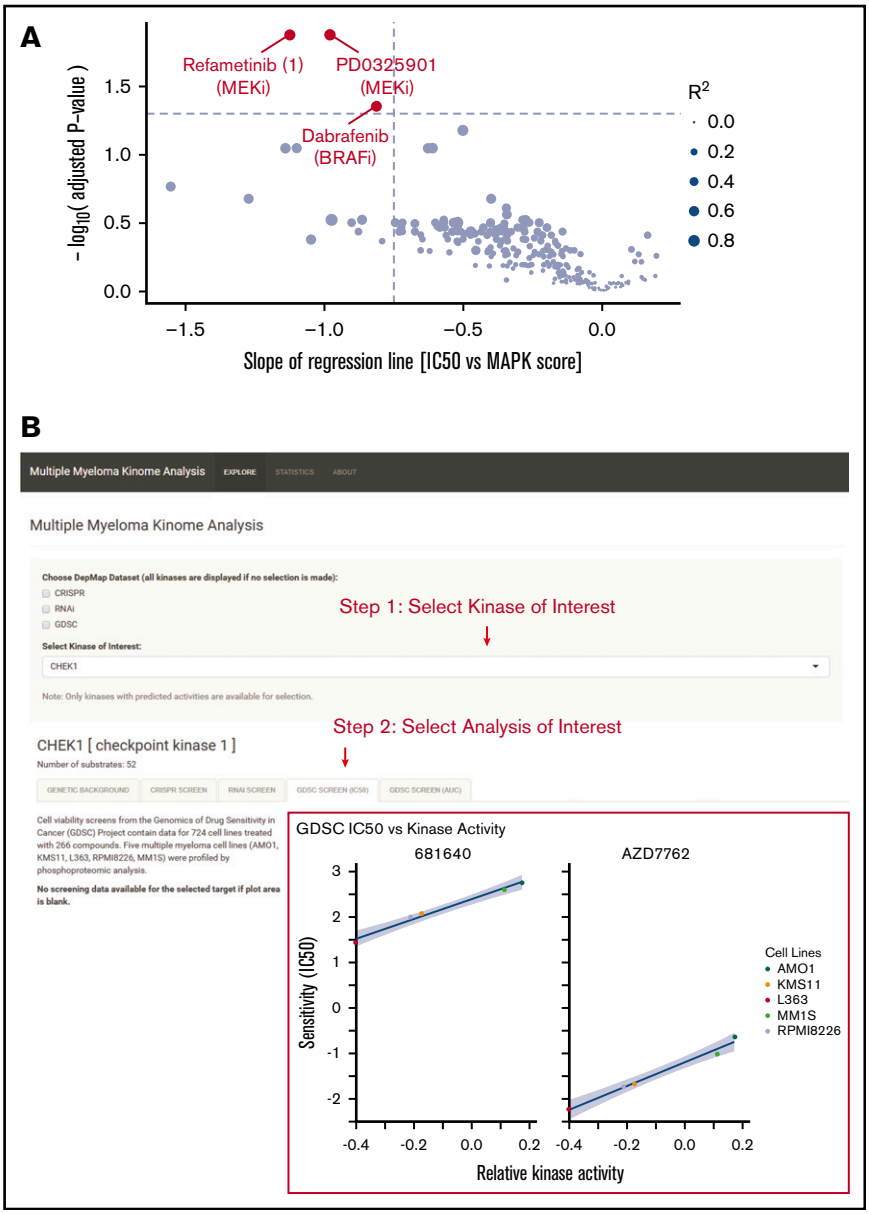

Figure 7. Integration of multiple data types for precision therapy in MM. (A) Volcano plot showing drug candidates for treating tumors with high predicted MAPK activity. Drug sensitivity data from Genomics of Drug Sensitivity in Cancer database (across 265 compounds tested) and MAPK scores from MM cell line transcriptome data (keatslab.org). *P* values are calculated based on the null hypothesis that no relationship exists between MAPK activity and inhibitor sensitivity. The 3 compounds with significant correlations between MAPK activity and drug sensitivity are highlighted in red. (B) Screenshot of the Multiple Myeloma Kinome Browser (https://tony-lin.shinyapps.io/depmap_app/). The example shows the integration of drug sensitivity data with phosphoproteome-based kinase activity predictions on MM cell lines for checkpoint kinase 1.

inhibitors, for example. Instead, we should focus on patients with high MAPK scores, regardless of *RAS* genotype. We found strongly increased MAPK scores in *RAS*-mutant cell lines vs WT, but not in patient samples, suggesting the tumor microenvironment in vivo may play an important role in modulating MAPK pathway activity. This hypothesis is in line with our prior evidence that interleukin-6 in the microenvironment strongly modulates MEK signaling and MM survival.[49] Furthermore, the high degree of intratumoral heterogeneity in MM creates particular hurdles for any therapy that may only eliminate specific subclones.[4] However, new approaches to directly target Ras,[12] in addition to existing strategies, may be particularly intriguing in these high-MAPK patients. We therefore suggest a functionally driven, as opposed to genotype-driven, approach to kinase inhibitor selection in MM. Though currently limited to cell lines, our publicly available tool at https://tony-lin.shinyapps.io/depmap_app/ will enable others to readily extract other kinase- and signaling-level relationships.

While we cannot definitively separate causation from correlation based on observational CoMMpass data, our results suggest that increased MAPK signaling is a driver of poor prognosis and that this increased signaling can be driven by various genomic lesions. In particular, the increased MAPK signaling and poorer outcomes driven by *NRAS* Q61 mutations are of interest. Q61 mutations in *RAS* (any isoform) may activate downstream signaling via complete abolition of guanosine triphosphate hydrolysis, as opposed to G12 and G13 mutations, which decrease but do not eliminate it.[13] This biochemistry may underpin the greater MAPK scores we find here for Q61 but does not necessarily explain the correlation between higher MAPK activity and poorer outcomes. Murine modeling in melanoma suggests similar increased potency of Q61 mutations,[50] and a minimal overexpression model of *NRAS* Q61 in WT *RAS* MM cell line (ANBL-6) confirmed increased proliferation with the introduction of this oncogene.[51] Further evaluating the effects of *NRAS* Q61 in myeloma is an intriguing path forward.

In summary, our results reveal the power of extending genomic studies to the dissection of functional changes within tumor cells using both phosphoproteomics and transcriptional data. We propose these findings will have broad implications in both MM precision medicine and the wider study of Ras biology.

Acknowledgments

The authors thank the MMRF for access to the CoMMpass data set and Kevin Shannon, Sandy Wong, Nina Shah, Jeffrey Wolf, and Tom Martin for the insightful discussions.

This work was supported by the Damon Runyon Cancer Research Foundation Dale Frey Breakthrough Award (DFS 14-15), the National Institutes of Health (National Cancer Institute grants K08CA184116 and R01CA226851; and National Institute of General Medical Sciences grant DP2OD022552), and the UCSF Stephen and Nancy Grand Multiple Myeloma Translational Initiative (A.P.W.); the MMRF Answer Fund and the National Institutes of Health (National Cancer Institute grant P30 CA138292) (L.H.B.); and American Cancer Society postdoctoral fellowship PF-17-109-1-TBG (B.G.B.). G.P.W. was supported in part by a training grant from the National Institutes of Health (National Human Genome Research Institute grant T32 HG000046). This work was funded in part by a grant from the Gordon and Betty Moore Foundation (GBMF 4552) (C.S.G.).

Authorship

Contribution: A.P.W. conceptualized the study; Y.-H.T.L., G.P.W., B.G.B., L.H.B., C.S.G., and A.P.W. contributed to methodology; Y.-H.T.L., G.P.W., and B.G.B. contributed to software, data curation, formal analysis, and visualization; Y.-H.T.L., M.C.M., M.M., and I.D.F. contributed to investigation; C.D. provided resources; Y.-H.T.L. and A.P.W. wrote the original draft; G.P.W., B.G.B., L.H.B., and C.S.G. reviewed and edited the manuscript; and C.S.G., L.H.B., and A.P.W. acquired funding.

Conflict-of-interest disclosure: A.P.W. has received past research funding from TeneoBio, Sutro BioPharma, and Quadriga BioSciences and is a member of the scientific advisory board and equity holder of Indapta Therapeutics and Protocol Intelligence. The remaining authors declare no competing financial interests.

The current affiliation for G.P.W. is Imaging Platform, Broad Institute of Harvard and MIT, Cambridge, MA.

ORCID profiles: Y.-H.T.L., 0000-0002-7157-4330; G.P.W., 0000-0002-0503-9348; B.G.B., 0000-0001-9810-3566; I.D.F., 0000-0003-4762-8762; C.S.G., 0000-0001-8713-9213; A.P.W., 0000-0002-7465-6964.

Correspondence: Arun P. Wiita, UCSF Department of Laboratory Medicine, 185 Berry St, Suite 290, San Francisco, CA 94107; e-mail: arun.wiita@ucsf.edu.

References

1. Bolli N, Avet-Loiseau H, Wedge DC, et al. Heterogeneity of genomic evolution and mutational profiles in multiple myeloma. *Nat Commun*. 2014;5(1):2997.
2. Chapman MA, Lawrence MS, Keats JJ, et al. Initial genome sequencing and analysis of multiple myeloma. *Nature*. 2011;471(7339):467-472.
3. Laganà A, Perumal D, Melnekoff D, et al. Integrative network analysis identifies novel drivers of pathogenesis and progression in newly diagnosed multiple myeloma. *Leukemia*. 2018;32(1):120-130.
4. Lohr JG, Stojanov P, Carter SL, et al; Multiple Myeloma Research Consortium. Widespread genetic heterogeneity in multiple myeloma: implications for targeted therapy. *Cancer Cell*. 2014;25(1):91-101.
5. Walker BA, Mavrommatis K, Wardell CP, et al. Identification of novel mutational drivers reveals oncogene dependencies in multiple myeloma. *Blood*. 2018;132(6):587-597.
6. Harding T, Baughn L, Kumar S, Van Ness B. The future of myeloma precision medicine: integrating the compendium of known drug resistance mechanisms with emerging tumor profiling technologies. *Leukemia*. 2019;33(4):863-883.
7. Casado P, Hijazi M, Britton D, Cutillas PR. Impact of phosphoproteomics in the translation of kinase-targeted therapies. *Proteomics*. 2017;17(6):1600235.
8. Ruprecht B, Lemeer S. Proteomic analysis of phosphorylation in cancer. *Expert Rev Proteomics*. 2014;11(3):259-267.
9. Casado P, Alcolea MP, Iorio F, et al. Phosphoproteomics data classify hematological cancer cell lines according to tumor type and sensitivity to kinase inhibitors. *Genome Biol*. 2013;14(4):R37.
10. Casado P, Wilkes EH, Miraki-Moud F, et al. Proteomic and genomic integration identifies kinase and differentiation determinants of kinase inhibitor sensitivity in leukemia cells. *Leukemia*. 2018;32(8):1818-1822.
11. Dermit M, Dokal A, Cutillas PR. Approaches to identify kinase dependencies in cancer signalling networks. *FEBS Lett*. 2017;591(17):2577-2592.
12. McCormick F. Targeting RAS directly. *Annu Rev Biochem*. 2018;2:81-90.
13. Simanshu DK, Nissley DV, McCormick F. RAS proteins and their regulators in human disease. *Cell*. 2017;170(1):17-33.
14. Cox AD, Fesik SW, Kimmelman AC, Luo J, Der CJ. Drugging the undruggable RAS: Mission possible? *Nat Rev Drug Discov*. 2014;13(11):828-851.
15. Li S, Balmain A, Counter CM. A model for RAS mutation patterns in cancers: finding the sweet spot. *Nat Rev Cancer*. 2018;18(12):767-777.
16. Newlaczyl AU, Hood FE, Coulson JM, Prior IA. Decoding RAS isoform and codon-specific signalling. *Biochem Soc Trans*. 2014;42(4):742-746.
17. Rasmussen T, Kuehl M, Lodahl M, Johnsen HE, Dahl IM. Possible roles for activating RAS mutations in the MGUS to MM transition and in the intramedullary to extramedullary transition in some plasma cell tumors. *Blood*. 2005;105(1):317-323.

18. Liu P, Leong T, Quam L, et al. Activating mutations of N- and K-ras in multiple myeloma show different clinical associations: analysis of the Eastern Cooperative Oncology Group Phase III Trial. *Blood*. 1996;88(7):2699-2706.

19. Chng WJ, Gonzalez-Paz N, Price-Troska T, et al. Clinical and biological significance of RAS mutations in multiple myeloma. *Leukemia*. 2008;22(12): 2280-2284.

20. Mulligan G, Lichter DI, Di Bacco A, et al. Mutation of NRAS but not KRAS significantly reduces myeloma sensitivity to single-agent bortezomib therapy. *Blood*. 2014;123(5):632-639.

21. Billadeau D, Liu P, Jelinek D, Shah N, LeBien TW, Van Ness B. Activating mutations in the N- and K-ras oncogenes differentially affect the growth properties of the IL-6-dependent myeloma cell line ANBL6. *Cancer Res*. 1997;57(11):2268-2275.

22. Rowley M, Van Ness B. Activation of N-ras and K-ras induced by interleukin-6 in a myeloma cell line: implications for disease progression and therapeutic response. *Oncogene*. 2002;21(57):8769-8775.

23. Xu J, Pfarr N, Endris V, et al. Molecular signaling in multiple myeloma: association of RAS/RAF mutations and MEK/ERK pathway activation. *Oncogenesis*. 2017;6(5):e337.

24. Lam C, Ferguson ID, Mariano MC, et al. Repurposing tofacitinib as an anti-myeloma therapeutic to reverse growth-promoting effects of the bone marrow microenvironment. *Haematologica*. 2018;103(7):1218-1228.

25. Way GP, Sanchez-Vega F, La K, et al. Machine learning detects pan-cancer ras pathway activation in the cancer genome atlas. *Cell Rep*. 2018;23: 172-180.e173.

26. Barwick BG, Neri P, Bahlis NJ, et al. Multiple myeloma immunoglobulin lambda translocations portend poor prognosis. *Nat Commun*. 2019;10(1):1911.

27. Soriano GP, Besse L, Li N, et al. Proteasome inhibitor-adapted myeloma cells are largely independent from proteasome activity and show complex proteomic changes, in particular in redox and energy metabolism. *Leukemia*. 2016;30(11):2198-2207.

28. Casado P, Rodriguez-Prados JC, Cosulich SC, et al. Kinase-substrate enrichment analysis provides insights into the heterogeneity of signaling pathway activation in leukemia cells. *Sci Signal*. 2013;6(268):rs6.

29. Samatar AA, Poulikakos PI. Targeting RAS-ERK signalling in cancer: promises and challenges. *Nat Rev Drug Discov*. 2014;13(12):928-942.

30. Müller E, Bauer S, Stühmer T, et al. Pan-Raf co-operates with PI3K-dependent signalling and critically contributes to myeloma cell survival independently of mutated RAS. *Leukemia*. 2017;31(4):922-933.

31. Guinney J, Ferté C, Dry J, et al. Modeling RAS phenotype in colorectal cancer uncovers novel molecular traits of RAS dependency and improves prediction of response to targeted agents in patients. *Clin Cancer Res*. 2014;20(1):265-272.

32. Merchant M, Moffat J, Schaefer G, et al. Combined MEK and ERK inhibition overcomes therapy-mediated pathway reactivation in RAS mutant tumors [published correction appears in *PLoS One*. 2018;13(1):e0192059]. *PLoS One*. 2017;12(10):e0185862.

33. Croonquist PA, Linden MA, Zhao F, Van Ness BG. Gene profiling of a myeloma cell line reveals similarities and unique signatures among IL-6 response, N-ras-activating mutations, and coculture with bone marrow stromal cells. *Blood*. 2003;102(7):2581-2592.

34. Xu J, Haigis KM, Firestone AJ, et al. Dominant role of oncogene dosage and absence of tumor suppressor activity in Nras-driven hematopoietic transformation. *Cancer Discov*. 2013;3(9):993-1001.

35. Tsherniak A, Vazquez F, Montgomery PG, et al. Defining a cancer dependency map. *Cell*. 2017;170:564-576.e516.

36. Steinbrunn T, Stühmer T, Gattenlöhner S, et al. Mutated RAS and constitutively activated Akt delineate distinct oncogenic pathways, which independently contribute to multiple myeloma cell survival. *Blood*. 2011;117(6):1998-2004.

37. Walker BA, Boyle EM, Wardell CP, et al. Mutational spectrum, copy number changes, and outcome: results of a sequencing study of patients with newly diagnosed myeloma. *J Clin Oncol*. 2015;33(33):3911-3920.

38. Schubert M, Klinger B, Klünemann M, et al. Perturbation-response genes reveal signaling footprints in cancer gene expression. *Nat Commun*. 2018;9(1): 20.

39. Kalff A, Spencer A. The t(4;14) translocation and FGFR3 overexpression in multiple myeloma: prognostic implications and current clinical strategies. *Blood Cancer J*. 2012;2(9):e89.

40. Katoh M, Nakagama H. FGF receptors: cancer biology and therapeutics. *Med Res Rev*. 2014;34(2):280-300.

41. Yang W, Soares J, Greninger P, et al. Genomics of Drug Sensitivity in Cancer (GDSC): a resource for therapeutic biomarker discovery in cancer cells. *Nucleic Acids Res*. 2013;41(Database issue):D955-D961.

42. Ghobrial IM, Siegel DS, Vij R, et al. TAK-228 (formerly MLN0128), an investigational oral dual TORC1/2 inhibitor: a phase I dose escalation study in patients with relapsed or refractory multiple myeloma, non-Hodgkin lymphoma, or Waldenström's macroglobulinemia. *Am J Hematol*. 2016;91(4): 400-405.

43. Rodrik-Outmezguine VS, Okaniwa M, Yao Z, et al. Overcoming mTOR resistance mutations with a new-generation mTOR inhibitor. *Nature*. 2016; 534(7606):272-276.

44. Needham EJ, Parker BL, Burykin T, James DE, Humphrey SJ. Illuminating the dark phosphoproteome. *Sci Signal*. 2019;12(565):eaau8645.

45. Steinbrunn T, Stühmer T, Sayehli C, Chatterjee M, Einsele H, Bargou RC. Combined targeting of MEK/MAPK and PI3K/Akt signalling in multiple myeloma. *Br J Haematol*. 2012;159(4):430-440.

46. Wong KY, Yao Q, Yuan LQ, Li Z, Ma ESK, Chim CS. Frequent functional activation of RAS signalling not explained by RAS/RAF mutations in relapsed/ refractory multiple myeloma. *Sci Rep*. 2018;8(1):13522.

47. Burgess MR, Hwang E, Mroue R, et al. KRAS allelic imbalance enhances fitness and modulates MAP kinase dependence in cancer. *Cell*. 2017;168: 817-829.e815.

48. Bielski CM, Donoghue MTA, Gadiya M, et al. Widespread selection for oncogenic mutant allele imbalance in cancer. *Cancer Cell*. 2018;34: 852-862.e854.

49. Gupta VA, Matulis SM, Conage-Pough JE, et al. Bone marrow microenvironment-derived signals induce Mcl-1 dependence in multiple myeloma. *Blood*. 2017;129(14):1969-1979.

50. Burd CE, Liu W, Huynh MV, et al. Mutation-specific RAS oncogenicity explains NRAS codon 61 selection in melanoma. *Cancer Discov*. 2014;4(12): 1418-1429.

51. Billadeau D, Jelinek DF, Shah N, LeBien TW, Van Ness B. Introduction of an activated N-ras oncogene alters the growth characteristics of the interleukin 6-dependent myeloma cell line ANBL6. *Cancer Res*. 1995;55(16):3640-3646.